

Convolutionally Coded Multicarrier DS-CDMA Systems in a Multipath Fading Channel—Part II: Narrow-Band Interference Suppression

Douglas N. Rowitch, *Member, IEEE*, and Laurence B. Milstein, *Fellow, IEEE*

Abstract—In Part I of this paper, a convolutionally encoded multicarrier asynchronous direct-sequence code-division multiple-access (DS-CDMA) system was proposed and compared to a classical single-carrier DS-CDMA system employing a RAKE receiver and the same convolutional code, in the presence of additive white Gaussian noise and multiple-access interference. This paper considers the additional impact of various forms of narrow-band interference on the performance of these two systems and the ability of the multicarrier system to effectively suppress the interference using the innate structure of its receiver. At roughly equivalent receiver complexity, results will demonstrate superior performance of the multicarrier system in the presence of such interference, without requiring the addition of a front-end interference suppression filter.

I. INTRODUCTION

THE capability of a conventional direct-sequence code-division multiple-access (DS-CDMA) receiver to combat the interference due to multiple-access users as well as the degradation due to fading is well known [1], [2]. However, in the presence of narrow-band interference (NBI) [e.g., partial-band interference (PBI)], a front-end interference suppression or notch filter is typically required, assuming that the interference power is sufficiently large [3]. Such instances of NBI may be intentional, as in various military applications, or may be unintentional, as in a commercial CDMA overlay scheme [4]. While such front-end filters may effectively suppress or reject the interfering signal, at the same time, they can distort the signal of the user-of-interest [3]. In addition, the interference filters come at the cost of additional receiver complexity.

While multicarrier systems proposed in [5]–[10] served to offer an alternative to the classical single-carrier DS-CDMA system as a means to realize a wide-band CDMA system, they

Paper approved by B. D. Woerner, the Editor for Wireless Spread Spectrum of the IEEE Communications Society. Manuscript received October 17, 1996; revised July 6, 1998. This work was supported in part by the National Science Foundation under Grant NCR-9213140 and in part by the Focused Research Initiative on Wireless Multimedia Networks under Grant DAAH04-95-1-0248. This paper was presented in part at the 1995 International Symposium on Information Theory, Whistler, BC, September 1995, in part at MILCOM'95, San Diego, CA, November 1995, and in part at MILCOM'96, McLean, VA, November 1996.

D. N. Rowitch was with the Department of Electrical and Computer Engineering, University of California at San Diego, La Jolla, CA 92093-0407 USA. He is now with Qualcomm Incorporated, San Diego, CA 92121 USA (e-mail: drowitch@qualcomm.com).

L. B. Milstein is with the Department of Electrical and Computer Engineering, University of California at San Diego, La Jolla, CA 92093-0407 USA (e-mail: milstein@ece.ucsd.edu).

Publisher Item Identifier S 0090-6778(99)08918-7.

were also devised with the objective of isolating various forms of NBI in the frequency-domain and selectively rooting out or attenuating the effects of the interference.

In this paper, we analyze the effects of Gaussian PBI and continuous wave tone interference (CWI) on both the proposed multicarrier system [5] and the reference single-carrier DS-CDMA system [1], [2]. In addition, we consider suboptimal combining techniques and faded versus unfaded performance of the multicarrier system, both in the presence and absence of NBI. It is presumed that the reader is familiar with Part I of this paper [5] and, as a result, replication of results from Part I will be kept at a minimum.

An overview of the organization of this paper is as follows. Section II identifies the received signal and briefly reviews system and channel assumptions. Section III presents a performance analysis of the system. In Section IV, we present numerical results of the system comparison. Finally, in Section V, we present the conclusions.

II. RECEIVED SIGNAL

As in Part I of this paper [5], we decompose the bandwidth of a single-carrier system

$$W_{SC} = (1 + \beta) \frac{1}{T_c} \quad (1)$$

into MR equiwidth disjoint frequency sub-bands of bandwidth

$$W_{MC} = \frac{W_{SC}}{MR} = (1 + \beta) \frac{1}{MRT_c} \quad (2)$$

where β is the rolloff factor of the respective chip wave-shaping filters ($0 < \beta \leq 1$), T_c is the chip duration of the single-carrier system, and MRT_c is the chip duration of the multicarrier system.

As in [5], we assume a slowly varying, frequency-selective Rayleigh fading channel with respect to the single-carrier system, such that L resolvable paths are experienced. The number of subcarriers MR is selected to be equal to L , such that each multicarrier sub-band fades nonselectively (flat) and independently [5].

Then, the received signal is identical to that of Part I [5], but with the addition of an NBI signal $n_J(t)$, as depicted (in the frequency-domain) in Fig. 1 (for the Gaussian PBI case).

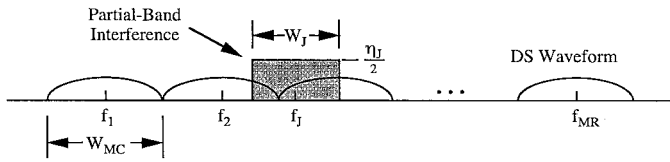


Fig. 1. PSD of PBI.

Thus, the received signal now takes the form

$$r(t) = \sum_{k=1}^{K_u} \left\{ \sqrt{2E_c} \sum_{n=-\infty}^{\infty} c_n^{(k)} h(t - nMRT_c - \tau_k) \cdot \sum_{\nu=1}^{MR} \alpha_{k,\nu} \left[a_{\nu,[n/N]}^{(k)} \cos(2\pi f_{\nu} t + \theta_{k,\nu}) + \tilde{a}_{\nu,[n/N]}^{(k)} \cdot \sin(2\pi f_{\nu} t + \theta_{k,\nu}) \right] \right\} + n_W(t) + n_J(t) \quad (3)$$

where $n_J(t)$ is the NBI with a power spectral density (PSD) of $S_{n_J}(f)$, and the remaining expressions are as specified in [5]. We use the same transmitter and receiver structure as specified in [5] and now consider the impact of the NBI on the performance of the desired user.

III. ANALYSIS

A. System Outputs due to NBI

Since the NBI, $n_J(t)$, is an additive signal and the receiver is a linear time-invariant structure, we will specify the receiver outputs due only to the interference and defer to [5] for the outputs corresponding to the signal-of-interest, the multiple-access interference (MAI), and the additive white Gaussian noise (AWGN).

The output, prior to sampling, from the in-phase and quadrature correlator branches at the ν th subcarrier frequency, $y_{\nu}^{(I)}(t)$ and $y_{\nu}^{(Q)}(t)$, in (12) and (13), respectively, from [5] are now augmented to include, respectively, the terms $J_{y_{\nu}}^{(I)}(t)$ and $J_{y_{\nu}}^{(Q)}(t)$. These latter expressions represent the signal due to the input NBI $n_J(t)$. The in-phase and quadrature outputs due to the NBI are

$$J_{y_{\nu}}^{(I)}(t) = Lp \left\{ n_{J_{\nu}}(t) \sqrt{2} \cos(2\pi f_{\nu} t + \theta_{1,\nu}) \right\} \quad (4)$$

and

$$J_{y_{\nu}}^{(Q)}(t) = Lp \left\{ n_{J_{\nu}}(t) \sqrt{2} \sin(2\pi f_{\nu} t + \theta_{1,\nu}) \right\}. \quad (5)$$

The term $n_{J_{\nu}}(t)$ represents the band-limited process obtained by convolving the NBI, $n_J(t)$, with the impulse response of the ν th bandpass chip filter and $Lp\{\cdot\}$ denotes a low-pass filter operation to remove double-frequency terms.

After sampling and despreading, the in-phase and quadrature correlator outputs, $Z_{\nu}^{(I)}$ and $Z_{\nu}^{(Q)}$, in (21) and (22) from [5] are now augmented to include, respectively, the terms $J_{Z_{\nu}}^{(I)}$ and $J_{Z_{\nu}}^{(Q)}$. These terms are given by

$$J_{Z_{\nu}}^{(I)} = \sum_{n'=0}^{N-1} c_{n'}^{(1)} J_{y_{\nu}}^{(I)}(n' MRT_c) \quad (6)$$

and

$$J_{Z_{\nu}}^{(Q)} = \sum_{n'=0}^{N-1} c_{n'}^{(1)} J_{y_{\nu}}^{(Q)}(n' MRT_c) \quad (7)$$

and represent, respectively, the in-phase and quadrature outputs due to the NBI.

For Gaussian PBI, it will be shown that $J_{Z_{\nu}}^{(I)}$ and $J_{Z_{\nu}}^{(Q)}$ are zero-mean Gaussian random variables. Similarly, for CWI, assuming the interfering tones experience frequency flat Rayleigh fading, it will be shown that $J_{Z_{\nu}}^{(I)}$ and $J_{Z_{\nu}}^{(Q)}$ are also zero-mean Gaussian random variables. It is reasonable to assume that the interference component, in either case, will be statistically independent from the other correlator output components. Thus, we may make use of the theoretical results stated in Part I [5], where we simply ascertain the additional variance contribution due to the NBI. Once the variances are augmented to reflect the NBI, the remaining results in Section III of Part I [5] may be applied directly to evaluate performance of the multicarrier system.

Therefore, drawing upon the results of Part I, the in-phase correlator output at the ν th subcarrier frequency, $Z_{\nu}^{(I)}$, when conditioned on the amplitude of the fading envelope and the transmitted code symbol, is approximately Gaussian, where the approximation is valid for a large number of users K_u and is perfect for $K_u = 1$. The conditional variance of $Z_{\nu}^{(I)}$, conditioned upon $\alpha_{1,\nu}$, is now given by

$$\begin{aligned} \text{var} \left\{ Z_{\nu}^{(I)} \mid \alpha_{1,\nu} \right\} &\equiv \left(\sigma_{\nu}^{(I)} \right)^2 \\ &= \text{var} \left\{ I_{Z_{\nu}}^{(I)} + N_{Z_{\nu}}^{(I)} + J_{Z_{\nu}}^{(I)} \mid \alpha_{1,\nu} \right\} \\ &= \text{var} \left\{ I_{Z_{\nu}}^{(I)} \mid \alpha_{1,\nu} \right\} + \text{var} \left\{ N_{Z_{\nu}}^{(I)} \mid \alpha_{1,\nu} \right\} \\ &\quad + \text{var} \left\{ J_{Z_{\nu}}^{(I)} \mid \alpha_{1,\nu} \right\}. \end{aligned} \quad (8)$$

The conditional variance for the NBI component $J_{Z_{\nu}}^{(I)}$ is derived in the following sections for both PBI and CWI.

B. Variance of PBI

In this case, $n_J(t)$ is Gaussian PBI and the corresponding correlator output, $J_{Z_{\nu}}^{(I)}$, is therefore a Gaussian random variable, by definition, since it represents the response of a linear time-invariant system to an input zero-mean Gaussian random process.

The conditional variance for the PBI component is given by

$$\begin{aligned} \text{var} \left\{ J_{Z_{\nu}}^{(I)} \mid \alpha_{1,\nu} \right\} &= \sum_{n'=0}^{N-1} \sum_{m'=0}^{N-1} c_{n'}^{(1)} c_{m'}^{(1)} R_{J_{y_{\nu}}} [(n' - m') MRT_c] \\ &= NR_{J_{y_{\nu}}}(0) + 2 \sum_{\ell=1}^{N-1} R_{J_{y_{\nu}}}(\ell MRT_c) \sum_{n'=\ell}^{N-1} c_{n'}^{(1)} c_{n'-\ell}^{(1)} \end{aligned} \quad (9)$$

where $R_{J_{y_{\nu}}}(\tau)$ is the autocorrelation function of $J_{y_{\nu}}^{(I)}(t)$ and is defined as the inverse Fourier transform of the PSD of $J_{y_{\nu}}^{(I)}(t)$

$$S_{J_{y_{\nu}}}(f) = \frac{1}{2} [S_{n_J}(f - f_{\nu}) + S_{n_J}(f + f_{\nu})] |H(f)|^2. \quad (10)$$

In (10), $S_{n_J}(f)$ is the PSD of the PBI, $n_J(t)$; it is given by

$$S_{n_J}(f) = \begin{cases} \frac{\eta_J}{2}, & f_J - \frac{W_J}{2} \leq |f| \leq f_J + \frac{W_J}{2} \\ 0, & \text{elsewhere} \end{cases} \quad (11)$$

and is graphically depicted in Fig. 1. In (11), f_J is the center frequency and W_J is the bandwidth (both in Hertz) of the PBI. The autocorrelation function, $R_{J_{y\nu}}(\tau)$, is derived explicitly in [10].

For the special case in which the PBI spans the entire ν th multicarrier sub-band, and assuming that a raised-cosine Nyquist filter is employed for pulse shaping, it can be shown that the variance of the in-phase PBI component is given by [10]

$$\text{var}\{J_{Z\nu}^{(I)}\} = NR_{J_{y\nu}}(0) = \frac{(\text{ISR})E_b}{2(1+\beta)\rho_J} \quad (12)$$

where $\rho_J \triangleq W_J/W_{\text{MC}}$ relates the bandwidth of the PBI to the bandwidth of a multicarrier sub-band, subject to $0 \leq \rho_J \leq MR$, and the interference-to-signal-power ratio (ISR) is defined as

$$\begin{aligned} \text{ISR} &\triangleq \frac{\text{interference power}}{\text{signal power}} \\ &= \frac{\eta_J W_J}{E_b/T} \\ &= \frac{\eta_J W_J}{E_b/(NMRT_c)} \\ &= \frac{\eta_J W_J}{E_b W_{\text{MC}}/(N(1+\beta))}. \end{aligned} \quad (13)$$

C. Variance of CWI

In this case, $n_J(t)$ is CWI. For one or more unmodulated tone interferers, we assume the following.

- The interference power is divided equally among the total number of tones Q .
- The tones experience slowly varying, frequency-nonsselective Rayleigh fading.

Assume an unmodulated tone interferer resides somewhere in the frequency sub-band of the ν th in-phase multicarrier sub-band. Define the received interference signal as

$$n_J(t) = \alpha_J \sqrt{2P_0} \cos(2\pi f_J t + \phi_J) \quad (14)$$

where P_0 is the power of the interfering tone, α_J is a Rayleigh distributed random variable with unit second moment, and ϕ_J is a uniformly distributed random variable on the interval $[0, 2\pi)$.

It can be shown [10] that the corresponding output of the in-phase correlator is given by

$$\begin{aligned} J_{Z\nu}^{(I)} &= \alpha_J H(\Delta f_J) \sqrt{P_0} \sum_{n'=0}^{N-1} c_{n'}^{(1)} \cos(2\pi \Delta f_J n' MRT_c + \Delta \phi_J) \\ &= H(\Delta f_J) \sqrt{P_0} \left\{ \xi_J^c \sum_{n'=0}^{N-1} c_{n'}^{(1)} \cos(2\pi \Delta f_J n' MRT_c) \right. \\ &\quad \left. - \xi_J^s \sum_{n'=0}^{N-1} c_{n'}^{(1)} \sin(2\pi \Delta f_J n' MRT_c) \right\} \end{aligned} \quad (15)$$

where $\Delta \phi_J \triangleq \phi_J - \theta_{1,\nu}$, $\Delta f_J \triangleq f_J - f_\nu$ is the frequency offset between the ν th subcarrier and the interfering tone (f_J), $H(f)$ is the transfer function of the chip wave-shaping filter, and where $\xi_J^c \triangleq \alpha_J \cos(\Delta \phi_J)$ and $\xi_J^s \triangleq \alpha_J \sin(\Delta \phi_J)$ are independently, identically distributed Gaussian random variables with zero mean and variance $1/2$. Since all of the quantities in (15) are deterministic except for ξ_J^c and ξ_J^s , it follows that $J_{Z\nu}^{(I)}$ is a Gaussian random variable with mean equal to zero.

We define the ISR as

$$\text{ISR} \triangleq \frac{\text{interference power}}{\text{signal power}} = \frac{P_0/Q}{E_b/T} = \frac{P_0/Q}{E_b/(NMRT_c)}. \quad (16)$$

Solving for P_0 and substituting into (15), we obtain the variance of $J_{Z\nu}^{(I)}$ as

$$\text{var}\left[J_{Z\nu}^{(I)}\right] = |H(\Delta f_J)|^2 \frac{(\text{ISR})E_b}{2QNMRT_c} [A_c^2(\Delta f_J) + A_s^2(\Delta f_J)] \quad (17)$$

where

$$A_s(x) \triangleq \sum_{n'=0}^{N-1} c_{n'}^{(1)} \sin(2\pi MRT_c n' x) \quad (18)$$

and

$$A_c(x) \triangleq \sum_{n'=0}^{N-1} c_{n'}^{(1)} \cos(2\pi MRT_c n' x). \quad (19)$$

For the special case of $\Delta f_J = 0$, where we assume the raised-cosine filter characteristic for $H(f)$, (17) simplifies to

$$\text{var}\left[J_{Z\nu}^{(I)}\right] = \frac{(\text{ISR})E_b}{2QN} \left(\sum_{n'=0}^{N-1} c_{n'}^{(1)} \right)^2. \quad (20)$$

D. Theoretical Comparison

We initially compare the variance of PBI from (12), assuming that the interference exactly spans the ν th multicarrier sub-band and does not affect any other sub-bands (i.e., $\rho_J = 1$), to the variance of CWI from (20), where we assume zero frequency offset ($\Delta f_J = 0$) and only one interfering tone (i.e., $Q = 1$). If the processing gain per subcarrier N of the multicarrier system is equal to the period P of the employed spreading sequence and if maximal-length pseudonoise (PN) sequences are used, then the sum, $C \triangleq \sum_{n'=0}^{N-1} c_{n'}^{(1)}$, will be equal to -1 , in which case the tone variance will be on the order of N times smaller than the PBI variance. However, due to the small processing gains per subcarrier and large number of supported users, the period of the spreading sequences will usually exceed the processing gain (i.e., $P \gg N$). In this case, it is readily observed that depending on the magnitude of the sum C , the variance due to CWI can be either larger or smaller than the variance due to PBI. For nonzero frequency offsets, the CWI variance may be yet larger. Therefore, we must condition on each distinct spreading sequence phase to accurately measure the performance of the system, for the CWI case.

Since each distinct spreading sequence phase implies a distinct variance in (17), we calculate both the bound on bit-

error rate (BER) due to the largest variance and the average of the bounds for all spreading sequence phases. Note that while the latter expression is no longer, strictly speaking, an upper bound, it nevertheless represents a reasonable measure of performance when removing conditioning on the spreading sequence.

E. Performance Analysis

We recall from Part I of this paper [5] that the correlator outputs corresponding to the i th convolutional code symbol are maximal-ratio combined to obtain

$$Z_i = \sum_{j=1}^{2R} g_{i,j} Z_{i,j} \quad (21)$$

where the adaptive gain coefficients (AGC's) $g_{i,j}$ are (perfect) estimates of the average fade amplitude divided by the variance in the (i,j) th multicarrier sub-band; specifically, it was shown that

$$g_{i,j} = \frac{\alpha_{1,\nu(i,j)}}{\sigma_{\nu(i,j)}^2}. \quad (22)$$

As stated in Part I [5], the AGC's have the effect of attenuating deeply fading correlator outputs such that the less faded terms have a greater contribution to the overall test statistic. Since the variance due to the AWGN and MAI will be the same in all multicarrier sub-bands, the presence of NBI will necessarily yield a larger variance in the affected subset of sub-bands. It is therefore evident that the AGC's will have a similar effect of attenuating the correlator outputs which are subject to NBI. Thus, the capability of the proposed system to suppress NBI is accomplished in a manner quite analogous to the mitigation of fading through diversity.

Since the transfer function bound developed in Part I of this paper [5] was capable of reflecting possibly unequal signal-to-interference-plus-noise ratios (SINR's), we may employ this bound directly with no additional modifications.

IV. NUMERICAL RESULTS

In Part I of this paper [5], we concluded that the single and multicarrier systems exhibited comparable performance at similar receiver complexity when in the presence of AWGN and MAI. In this section, we continue the comparison with the introduction of additive NBI. In addition, we consider the effect of suboptimal combining techniques (e.g., equal-gain combining) on multicarrier system performance. Finally, we examine faded versus unfaded performance of a multicarrier system.

A. System Comparison—PBI

To demonstrate the inherent NBI suppression effect, we compare a multicarrier system and a single-carrier system, both using a rate 1/8 code of constraint length $K = 7$ (64 states); the number of users is fixed at 100 and E_b/η_0 is fixed at 7 dB. In Fig. 2, the Gaussian PBI spans the third and fourth slots of the 16 multicarrier frequency sub-bands, and we plot the performance versus the ISR. Both upper bounds

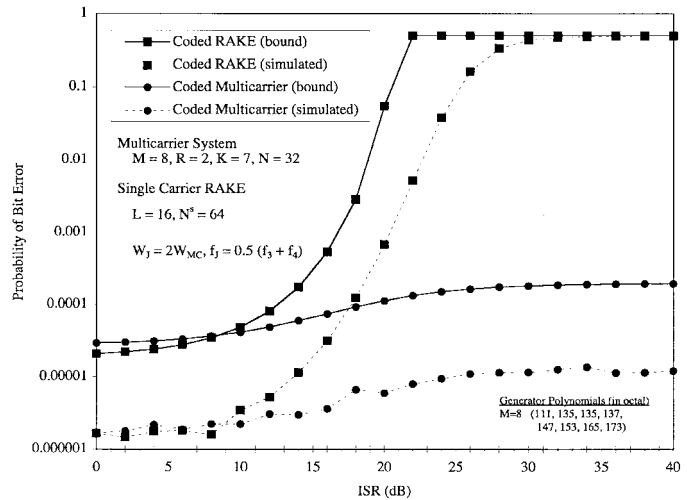


Fig. 2. BER (upper bound and simulated) versus ISR (dB), for $E_b/\eta_0 = 7$ dB and $K_u = 100$. PBI spans the third and fourth of the 16 multicarrier sub-bands. Illustrates the sensitivities of the two systems to increasing interference power. Demonstrates the interference suppression capability inherent to the multicarrier system design. The simulated results confirm the theoretical bounds.

and simulated results confirm the relative sensitivities of the two systems to the interference power. Once the ISR exceeds 10–12 dB, the performance of the single-carrier system quickly degrades.¹ The multicarrier system, on the other hand, is relatively insensitive to the strength of the interference.

As typically seen with such bounding techniques, the bounds are weak at high BER's (due to the union bound) and roughly an order of magnitude off at BER's of interest (due to the Chernoff bound). Note that in the simulation, perfect interleaving was assumed, perfect channel state information was assumed, and up to 10^8 data bits were simulated per simulation step (e.g., per E_b/η_0 level), stopping once 1000 bit errors were encountered. We assumed the use of maximal-length PN spreading sequences with periods exceeding the subcarrier processing gain, N .

In Figs. 3 and 4, we depict the BER as a function of E_b/η_0 and K_u , respectively, for ISR values $-\infty$, 10 and 20 dB, where the PBI is still assumed to span the third and fourth multicarrier sub-bands. In both figures, with no PBI (ISR = $-\infty$ dB), we see that the RAKE system slightly outperforms the multicarrier system, as discussed in Part I of this paper [5]. We see virtually identical performance at an ISR of 10 dB, and the multicarrier system is a clear winner at an ISR of 20 dB.

We now consider the behavior of an $M = 8$, $R = 2$ (16 subcarrier) system as we vary both the center frequency (f_j) and bandwidth (W_j) of the PBI. In Fig. 5, we vary the center frequency of the PBI for three different PBI bandwidths while fixing the ISR at either 10 or 20 dB. The interference bandwidths are expressed as multiples of a multicarrier sub-band bandwidth, $\rho \cdot W_{MC}$, for $\rho = 1, 3$, and 6. At an ISR of 20 dB, the notable conclusions one draws from this figure are as follows.

¹Of course, performance will improve with the addition of an interference suppression filter, but at the expense of added complexity.

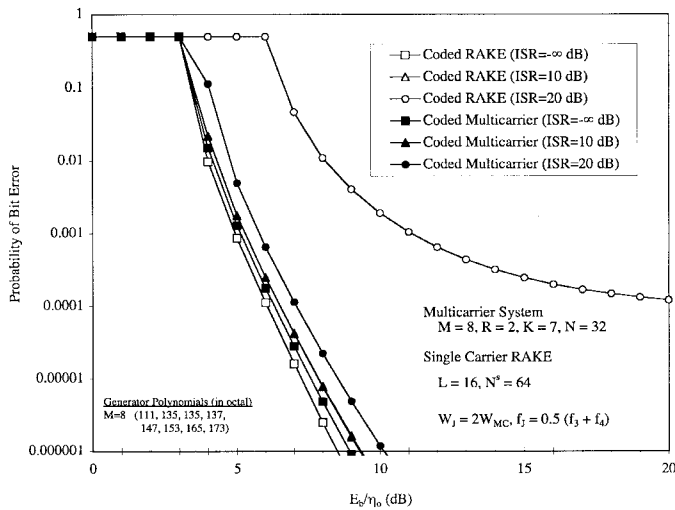


Fig. 3. BER upper bound versus E_b/η_0 (dB), with PBI, for $K_u = 100$. Examines the single-carrier and multicarrier system performance for a fixed user load and varying signal-to-noise ratio (SNR) at several ISR levels. Demonstrates the sensitivity of the single-carrier system to the interference and its inability to compensate by increasing signal power.

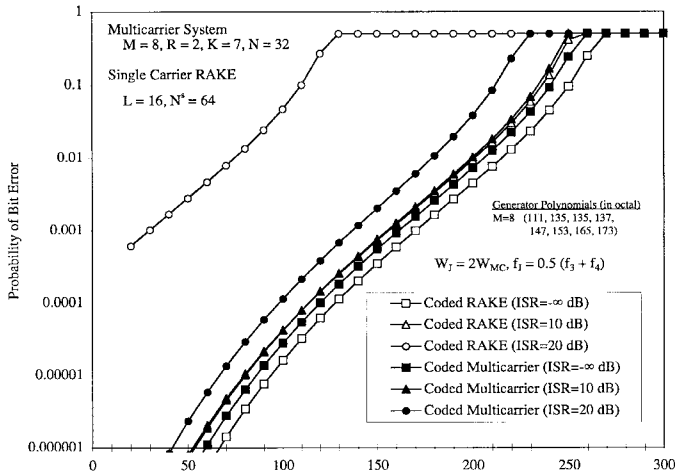


Fig. 4. BER upper bound versus K_u , with PBI, for $E_b/\eta_0 = 7$ dB. Examines the single-carrier and multicarrier system performance for a fixed SNR and varying user load at several ISR levels. Demonstrates the capacity gains realized by the multicarrier implementation, especially when the ISR is large.

- 1) The wider the interference bandwidth, the greater the degradation in performance.
- 2) For a fixed interference bandwidth $\rho \cdot W_{MC}$, the performance is best when the interference spans ρ sub-bands and is worst when it is centered about $\rho + 1$ sub-bands.
- 3) There is no significant sensitivity to the PBI center frequency, other than conclusion 2, mentioned above.²

At an ISR of 10 dB, although we see the same three effects as at 20 dB, the magnitude of these effects are, by comparison, minimal. Therefore, at smaller ISR values, the multicarrier systems is relatively insensitive to both the center frequency and bandwidth of the PBI.

²In [7] and [8], there was found to be a sensitivity to f_J , and this was explained by the minimum free distance error event of the code. This sensitivity has been effectively mitigated through the introduction of repetition coding of each convolutional code symbol.

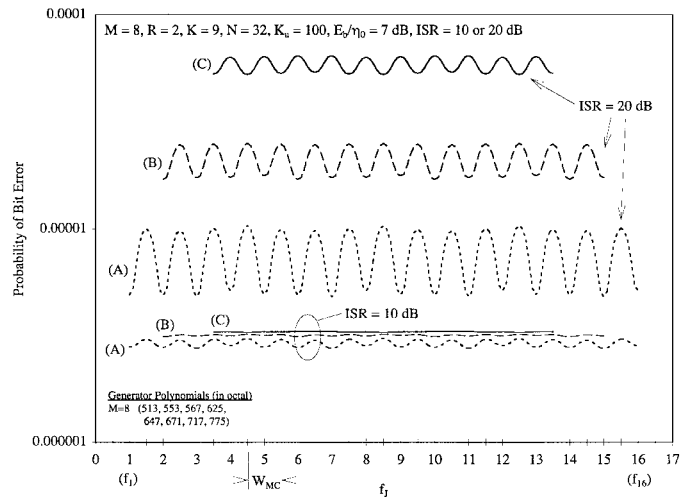


Fig. 5. BER upper bound versus f_J , for $E_b/\eta_0 = 7$ dB and $K_u = 100$. For several PBI bandwidths: (A) $W_J = W_{MC}$, (B) $W_J = 3W_{MC}$, and (C) $W_J = 6W_{MC}$, we plot the effects on the BER as the PBI center frequency varies across the allocated spectrum for several discrete ISR values.

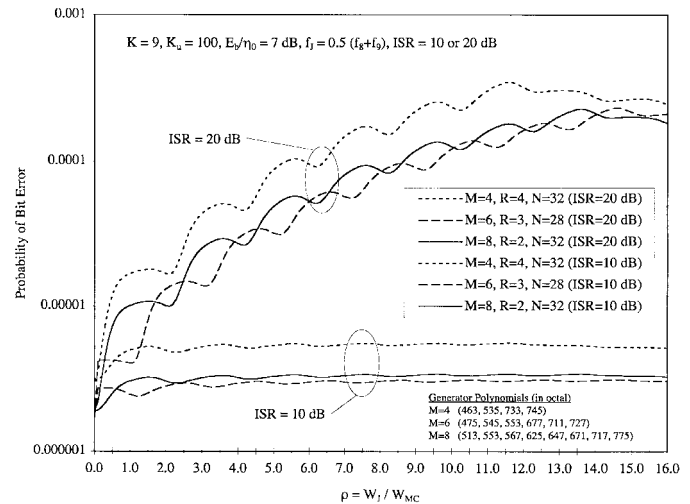


Fig. 6. BER upper bound versus W_J , for $E_b/\eta_0 = 7$ dB and $K_u = 100$. With the PBI center frequency fixed at the center of the allocated spectrum, we plot the effects on the BER as the PBI bandwidth grows. In this plot, we consider several discrete ISR values and several combinations of M and R , such that $MR \approx 16$.

Next, we fix f_J at the center-most frequency of the system bandwidth and allow W_J to vary for $(M = 4, R = 4)$, $(M = 6, R = 3)$, and $(M = 8, R = 2)$ multicarrier systems (where $MR \approx 16$), again with the ISR fixed at either 10 or 20 dB. In Fig. 6, we see a similar result at an ISR of 20 dB, in that the performance tends to be worst when the PBI bandwidth is largest. For smaller ISR values, the performance is relatively insensitive to the interference bandwidth. It is difficult to glean much else from this figure, since the convolutional codes and their inherent distance properties are different for each multicarrier system.

B. System Comparison—CWI

In this section, we contrast multicarrier system performance in the presence of Gaussian PBI with its performance when operating against pure tone interference. We assume the use of maximal-length PN spreading sequences of period $P = 2047$.

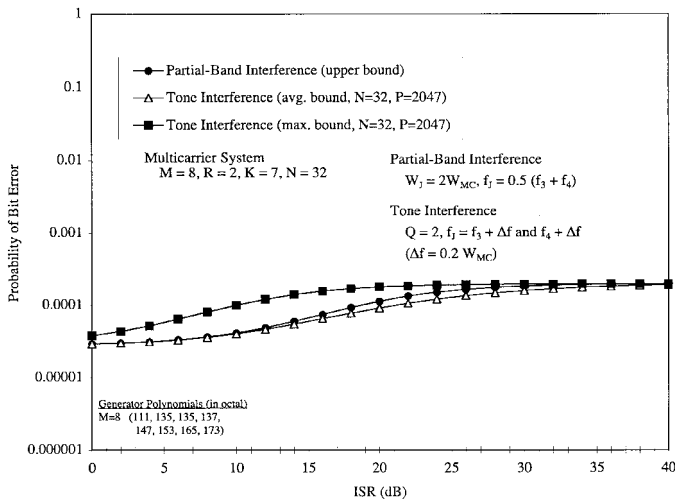


Fig. 7. BER upper bound versus ISR (dB), PBI, or CWI, with frequency offset, for $E_b/\eta_0 = 7$ dB and $K_u = 100$. Compares the relative degradation caused by these two types of interference and how the multicarrier system is capable of combating tone interference as successfully as it does PBI.

In Fig. 7, we examine BER versus ISR, with identical parameters as for Fig. 2. In this case, the PBI spans the third and fourth slots of the 16 multicarrier frequency subbands, whereas the two interfering tones are offset by $\Delta f_J = 0.2 \cdot W_{MC}$ Hz from the third and fourth subcarrier frequencies. The curves due to PBI and those due to the averaged (i.e., unconditional) upper bound for tone interference are very close to each other, with the PBI causing slightly more degradation in performance. This result is somewhat appealing in that it suggests that the multicarrier system combats interference both with little inherent structure (Gaussian PBI) and much structure (CWI), yielding highly similar performance in either case. This behavior is consistent with past efforts which examined the effects of tone and noise jamming on DS spread-spectrum systems [12], [13].

C. Suboptimal Combining

The AGC's used by the maximal-ratio combiners as proposed in Section III of Part I of this paper [5] are repeated in (22). To calculate these gain coefficients requires the estimation of both the mean and variance of a set of samples during which the channel is essentially constant. If NBI is not a concern, then the estimate of the variance in the denominator of (22) may be omitted (since the variance will be the same in all sub-bands). We denote the parameters to be estimated as μ (mean) and σ^2 (variance). It can be shown that classical, unbiased, maximum-likelihood estimates of these parameters, given that the sample data is Gaussian, will have variances [14]

$$\text{var}[\hat{\mu}] = \sigma^2/n \quad (23)$$

and

$$\text{var}[\hat{\sigma}^2] = 2\sigma^4/(n-1) \quad (24)$$

where n is the number of samples used to form the estimate. Because the latter variance is larger than the former, it may be of interest to consider the impact on performance if the denominator in (22) is omitted. In this case, the gain

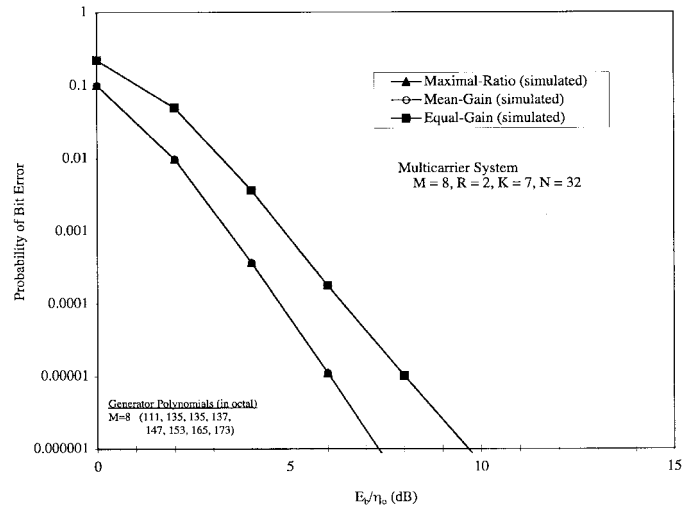


Fig. 8. Simulated BER versus E_b/η_0 (dB), suboptimal combining, no PBI, for $K_u = 100$. Examines the effects of suboptimal combining in the absence of NBI. Illustrates the performance penalty due to using equal-gain combining.

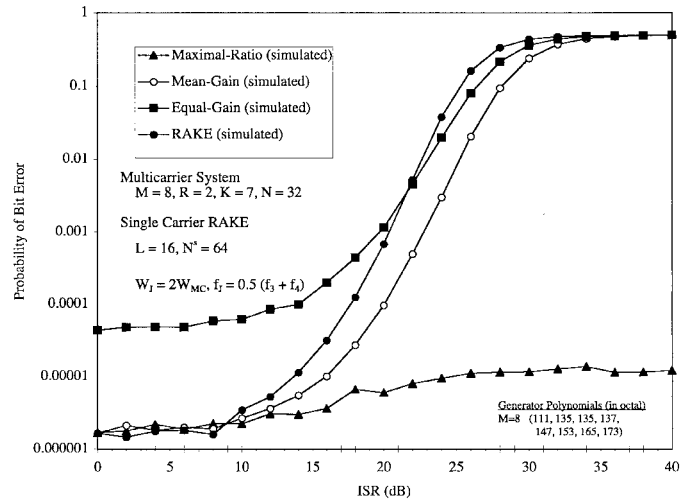


Fig. 9. BER versus ISR (dB), suboptimal combining, with PBI, for $E_b/\eta_0 = 7$ dB and $K_u = 100$. Examines the effects of suboptimal combining in the presence of NBI. Illustrates the performance penalty due to using mean-gain or equal-gain combining.

coefficients will still tend to attenuate deeply fading diversity branches, but will fail to attenuate branches experiencing NBI. We denote these hybrid gain coefficients as “mean-gain” coefficients. It is also of interest to examine the degradation in performance if gain factors are omitted entirely (i.e., equal-gain combining). Unfortunately, the bounding techniques used in Part I fail for these alternative schemes, so we rely on simulations to draw comparisons.

In Fig. 8, we plot simulated BER versus E_b/η_0 in the absence of NBI. In this case, the maximal-ratio and “mean-gain” methods will yield identical results, whereas the use of equal-gain combining results in a 1.5-dB loss at a BER of 10^{-3} . It should be noted, however, that the assumption of perfect estimation renders the maximal-ratio curve optimistic.

More interesting to note is the comparison of these schemes in the presence of PBI. In Fig. 9, we examine simulated BER versus ISR, where the maximal-ratio multicarrier and single-

carrier results are the same as seen in Fig. 2. We see that all techniques yield systems that are relatively insensitive to PBI, when the ISR is less than about 10 dB, noting, however, that the equal-gain system is over an order of magnitude worse in BER. Once the ISR exceeds 10 dB, the equal-gain, “mean-gain,” and RAKE systems quickly degrade, whereas the maximal-ratio system remains insensitive to the interference. At a BER of 10^{-3} , the equal-gain system is about 0.5 dB worse, and the “mean-gain” system is about 2 dB better than the single-carrier system. The single-carrier system is seen to degrade at a relatively quicker rate because the PBI affects all code symbols, whereas in the multicarrier systems, only a subset of code symbols see an impact.

If R (the repetition code parameter) is made large enough, hybrid multicarrier transceivers can be considered, which inhibit transmission in sub-bands experiencing a large degree of NBI (say above $\text{ISR} = 10$ dB). The receiver would only correlate and combine signals from sub-bands that are not inhibited. Given such a scheme, the suboptimal equal-gain and “mean-gain” weighting schemes become viable alternatives.³ This scheme would be particularly advantageous for a CDMA overlay [5] from the standpoint of minimizing the interference to narrow-band microwave users caused by the CDMA system.

D. Unfaded Performance

In this section, we investigate the unfaded performance of a multicarrier system. In this case, the diversity structure imposed by the parameter R will yield no improvement in performance, except insofar as it serves to mitigate NBI. If we follow the derivations in Section III of Part I of this paper [5], we note that for the unfaded case, the in-phase and quadrature correlator outputs will be conditionally, asymptotically, jointly Gaussian, conditioned only on the transmitted code symbols. The AGC’s in (22) will effectively simplify to

$$g_{i,j} = \frac{1}{\sigma_{\nu(i,j)}}. \quad (25)$$

There will be no change in the maximum-likelihood branch or path metrics; however, the Chernoff bound used to evaluate system performance will differ for the unfaded case. It can be shown [10] that the Chernoff bound on $P(d_1, d_2, \dots, d_M)$ (from [5]), for the unfaded case, is given by

$$P(d_1, d_2, \dots, d_M) < \prod_{i=1}^M \left\{ \prod_{j=1}^{2R} e^{-\bar{\gamma}_{i,j}} \right\}^{d_i} = \prod_{i=1}^M \left\{ e^{-\sum_{j=1}^{2R} \bar{\gamma}_{i,j}} \right\}^{d_i} \quad (26)$$

where $\bar{\gamma}_{i,j}$ is given by (44) in Part I of this paper. Finally, we may evaluate the union bound on the probability of first-event error and the probability of bit error, respectively, via (46) from [5], with P_i replaced by

$$P'_i \triangleq e^{-\sum_{j=1}^{2R} \bar{\gamma}_{i,j}}, \quad i = 1, 2, \dots, M. \quad (27)$$

³Of course, determining which sub-bands to inhibit may require a statistic similar to the variance estimate, and this scheme might require the additional overhead of a feedback control protocol.

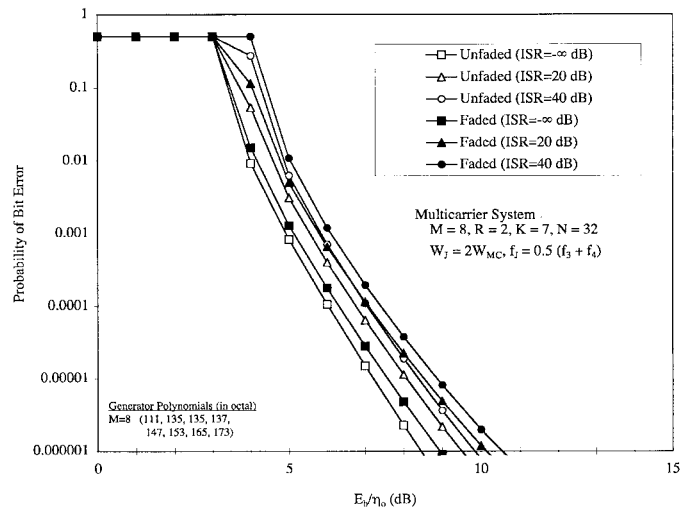


Fig. 10. BER upper bound versus E_b/η_0 (dB), faded and unfaded, for $K_u = 100$. Compares faded and unfaded multicarrier systems with a fixed user load and varying SNR at several discrete ISR levels. Illustrates the loss due to fading and the extent to which the coding and diversity combining combat the fading.

Tighter bounds are possible for the AWGN channel [15, Appendix 5A]. We opt, instead, to use the weaker bounds derived above to facilitate comparison with bounds developed for the faded case.

Comparing the Chernoff bound on the probability of symbol error for the i th convolutional code symbol, given by (47) from Part I and (27), for the faded and unfaded cases, respectively, one measure of the loss due to fading is given by

$$\frac{P'_i}{P_i} = \frac{P_s(\text{unfaded})}{P_s(\text{faded})} = \frac{e^{-\sum_{j=1}^{2R} \bar{\gamma}_{i,j}}}{\prod_{j=1}^{2R} \frac{1}{1 + \bar{\gamma}_{i,j}}} = \prod_{j=1}^{2R} (1 + \bar{\gamma}_{i,j}) e^{-\bar{\gamma}_{i,j}} \quad (28)$$

where P_s denotes the probability of a symbol error. In the absence of NBI, the average SINR terms, $\bar{\gamma}_{i,j}$, will be equal for all i and j . Denoting this common value by $\bar{\gamma}$, we have

$$\frac{P'_i}{P_i} = (1 + \bar{\gamma})^{2R} e^{-2R\bar{\gamma}}. \quad (29)$$

When one considers the approximation $e^x \approx 1 + x$, which is valid for $|x| \ll 1$, it can be seen that the ratio in (29) will be close to 1 for moderate SINR values. This implies similar performance bounds and, indeed, similar performance. As an example, consider an $M = 8$, $R = 2$ multicarrier system, with no MAI and with $E_b/\eta_0 = 7$ dB. For this case, since $\bar{\gamma} = (1/32)E_b/\eta_0 = 1.95$ dB. Evaluating (29) for this example yields

$$\frac{P'_i}{P_i} = (1 + \bar{\gamma})^4 e^{-4\bar{\gamma}} = 0.957. \quad (30)$$

In fact, for this case, $P_i = 0.559$, whereas $P'_i = 0.535$, and thus, we would expect similar performance in both the faded and unfaded cases, with a slight loss due to fading. When we include MAI and NBI, the average SINR values, $\bar{\gamma}_{i,j}$,

become smaller yet, rendering the above approximation more accurate. It is only at high values of E_b/η_0 or small bandwidth expansion factors, MR , that the loss due to fading will be significant. Thus, for R sufficiently large, the use of strong codes with a large degree of bandwidth expansion implies a relatively small loss due to fading at low to moderate values of E_b/η_0 .

In Fig. 10, we depict faded and unfaded multicarrier system performance as a function of E_b/η_0 , for ISR values $-\infty$, 20 and 40 dB, where the PBI is still assumed to span the third and fourth multicarrier sub-bands. We witness, regardless of the ISR value or the desired BER, about a 0.5-dB loss in SNR, due to fading. Thus, with and without PBI, the multicarrier system effectively combats Rayleigh fading, through its use of diversity and coding.

V. CONCLUSION

In Parts I and II of this paper, we proposed a new way of realizing a wide-band CDMA system that embodies robustness to multipath fading and mitigation of both MAI and NBI. At greater transmitter complexity, but roughly the same receiver complexity as a classical single-carrier DS-SS system, the multicarrier system was shown to exhibit an NBI suppression effect without the need for a front-end interference suppression or notch filter. Hybrid schemes involving suboptimal combining techniques were also considered to reduce complexity, and the corresponding performance penalties were assessed. The multicarrier system, consequently, represents a viable structure for a CDMA overlay scheme as described in [4].

REFERENCES

- [1] G. L. Turin, "Introduction to spread-spectrum antimultipath techniques and their application to urban digital radio," in *Proc. IEEE*, vol. 68, pp. 328–353, Mar. 1980.
- [2] R. L. Pickholtz, D. L. Schilling, and L. B. Milstein, "Theory of spread-spectrum communications—A tutorial," *IEEE Trans. Commun.*, vol. COM-30, pp. 855–884, May 1982.
- [3] L. B. Milstein, "Interference rejection techniques in spread spectrum communications," in *Proc. IEEE*, vol. 76, pp. 657–671, June 1988.
- [4] L. B. Milstein, D. L. Schilling, R. L. Pickholtz, V. Erceg, M. Kullback, E. G. Kanterakis, D. S. Fishman, W. H. Biederman, and D. C. Salerno, "On the feasibility of a CDMA overlay for personal communications networks," *IEEE J. Select. Areas Commun.*, vol. 10, pp. 655–667, May 1992.
- [5] D. N. Rowitch and L. B. Milstein, "Convolutionally coded multicarrier DS-SS systems in a multipath fading channel—Part I: Performance analysis," *IEEE Trans. Commun.*, vol. 47, pp. 1570–1592, Oct. 1999.
- [6] S. Kondo and L. B. Milstein, "On the performance of multicarrier DS-SS systems," *IEEE Trans. Commun.*, vol. 44, pp. 238–246, Feb. 1996.
- [7] D. N. Rowitch and L. B. Milstein, "Coded multicarrier code division multiple access," in *Proc. 1995 Int. Symp. Information Theory*, Whistler, BC, Canada, Sept. 1995, p. 23.
- [8] ———, "Convolutional coding for direct sequence multicarrier CDMA," in *Proc. MILCOM'95*, San Diego, CA, Nov. 1995, pp. 55–59.
- [9] ———, "Coded multicarrier DS-SS in the presence of partial band interference," in *Proc. MILCOM'96*, McLean, VA, Nov. 1996, pp. 204–209.
- [10] D. N. Rowitch, "Convolutional and turbo coded multicarrier direct sequence CDMA, and applications of turbo codes to hybrid ARQ communication systems," Ph.D. dissertation, Univ. of California-San Diego, La Jolla, CA, June 1998.
- [11] A. J. Viterbi, "Convolutional codes and their performance in communication systems," *IEEE Trans. Commun.*, vol. COM-19, pp. 751–772, Oct. 1971.
- [12] D. L. Schilling, L. B. Milstein, R. L. Pickholtz, and R. W. Brown, "Optimization of the processing gain of an M -ary direct sequence spread spectrum communication system," *IEEE Trans. Commun.*, vol. COM-28, pp. 1389–1398, Aug. 1980.
- [13] M. K. Simon, J. K. Omura, R. A. Scholtz, and B. K. Levitt, *Spread Spectrum Communications Handbook*. New York: McGraw-Hill, 1994.
- [14] H. Cramér, *Mathematical Methods of Statistics*. Princeton, NJ: Princeton Univ. Press, 1946.
- [15] A. J. Viterbi, *CDMA: Principles of Spread Spectrum Communication*. Reading, MA: Addison-Wesley, 1995.

Douglas N. Rowitch (S'94–M'98), for a photograph and biography, see p. 1582 in the October 1999 issue of this TRANSACTIONS.

Laurence B. Milstein (S'66–M'68–SM'77–F'85), for a photograph and biography, see p. 88 in the January 1999 issue of this TRANSACTIONS.